Zero-Bias Tunneling Anomaly in a Clean 2D Electron Gas Caused by Smooth Density Variations

T. A. Sedrakyan, E. G. Mishchenko, and M. E. Raikh
Department of Physics, University of Utah, Salt Lake City, Utah 84112, USA
(Received 17 June 2007; published 16 November 2007)

We show that smooth variations, $\delta n(\mathbf{r})$, of the local electron concentration in a clean 2D electron gas give rise to a zero-bias anomaly in the tunnel density of states, $\nu(\omega)$, even in the absence of scatterers, and thus, without the Friedel oscillations. The energy width, ω_0, of the anomaly scales with the magnitude, δn, and characteristic spatial extent, D, of the fluctuations as $(\delta n/D)^{2/3}$, while the relative magnitude $\delta\nu/\nu$ scales as $(\delta n/D)$. With increasing ω, the averaged $\delta\nu$ oscillates with ω. We demonstrate that the origin of the anomaly is a weak curving of the classical electron trajectories due to the smooth inhomogeneity of the gas. This curving suppresses the corrections to the electron self-energy which come from the virtual processes involving two electron-hole pairs.

DOI: 10.1103/PhysRevLett.99.206405 PACS numbers: 71.10.Pm, 73.40.Gk, 73.23.Hk

Introduction.—The origin of a zero-bias anomaly in the tunnel density of states of disordered metals had been traced [1] to the enhancement of the electron-electron interactions, caused by their diffusive motion. In two dimensions, the relative correction, $\delta\nu(\omega)/\nu$, to the tunnel density of states due to this enhancement is equal to $(1/2\pi E_F\tau)\ln(E_F^4\tau^3/\omega)\ln(\omega\tau)$ [2]. Here $\nu = m/\pi\hbar^2$ is the bare density of states, E_F is the Fermi energy, m is the electron mass, and τ is the scattering time. Diffusive description applies in the energy domain $\omega \lesssim 1/\tau$. In clean samples with mobility $\sim 10^6$ cm^2/Vs this domain is very narrow, $\sim 10^{-3}$ meV. In fact, as it was demonstrated in Ref. [3], the 2D zero-bias anomaly extends into the ballistic regime $\omega \gg 1/\tau$ and essentially retains its functional form. Virtual processes, responsible for the anomaly in this regime, involve one impurity and one electron-electron scattering with either small, $q \ll k_F$, or large, $q \approx 2k_F$, momentum transfer.

The relative magnitude of the interaction correction, $\delta\nu/\nu$, falls off with increasing the electron mobility. As experimental samples become progressively cleaner, the question arises whether the tunnel density of states in the absence of impurities exhibits a zero-bias anomaly. This issue was first addressed in Ref. [4]; the calculation in this paper predicted the interaction correction of the form $\delta\nu(\omega)/\nu \propto \omega$. However, later analysis [5] indicated that, for a finite interaction range, d, the singular behavior, $\delta\nu/\nu = \omega/4E_F$, of the correction saturates at $\omega \lesssim v_F/d$, where v_F is the Fermi velocity.

In the present Letter we identify a new mechanism of a zero-bias anomaly, which is at work for finite-range interactions and in the absence of impurities. Namely, we show that a narrow feature in $\delta\nu(\omega)$ emerges as a result of weak, long-scale variations of the electron density, $n(\mathbf{r})$, which are generic for high-mobility samples. Our main idea is that the high-order electron-electron scattering processes in a clean 2D gas, i.e., the processes that involve more than one virtual electron-hole pair, are anomalously sensitive to the variations of $n(\mathbf{r})$. An example of such process with two virtual pairs is shown in Fig. 1(a). The diagram in Fig. 1(a) with three interaction lines describes creation of an electron-hole pair, which is subsequently rescattered into another pair, and, finally, annihilated. As was first pointed out in Ref. [6], the momenta of states involved in this process are strongly correlated; namely, they are either almost parallel or almost antiparallel to each other. It is this correlation that is affected by the spatial inhomogeneity. The resulting suppression of the contributions of the higher-order processes, like that shown in Fig. 1(a), to the self-energy, gives rise to a zero-bias anomaly. Lack of strong correlation in the momenta directions in excitation of a single pair implies that second-order processes do not contribute to the anomaly.

Qualitative consideration.—The degree of alignment of the momenta of states in the diagram Fig. 1(a) can be established from the following consideration. Denote with $\mathbf{Q}$ and $\mathbf{P}$ the momenta transfer in the course of creation and subsequent rescattering of the electron-hole pair. Then the conditions that the energies of all electrons and holes, constituting the pairs, are close to the Fermi surface can be presented as $|\epsilon_{\mathbf{q}_1+\mathbf{Q}/2} - E_F| \sim |\epsilon_{\mathbf{q}_1-\mathbf{Q}/2} - E_F| \sim \omega$, and $|\epsilon_{\mathbf{q}_1-\mathbf{P}+\mathbf{Q}/2} - E_F| \sim |\epsilon_{\mathbf{q}_1+\mathbf{P}-\mathbf{Q}/2} - E_F| \sim \omega$, where $\epsilon_q = q^2/2m$ and ω is the energy of the pair. The above conditions can be met when either $|\mathbf{Q}|$ and $|\mathbf{P}|$ are both small (much smaller than k_F) or when one of them is small, while the other is close to $2k_F$. For concreteness, we consider the case $|\mathbf{Q}| \approx 2k_F$, $|\mathbf{P}| \ll k_F$. Then it follows from the first condition that $|\mathbf{q}_1| \ll k_F$ and that $\mathbf{q}_1 \cdot \mathbf{Q} \sim \omega k_F/v_F$.

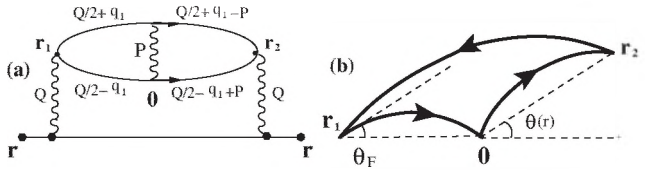

FIG. 1. (a) A diagram describing a virtual process of creation, rescattering, and annihilation of the electron-hole pair; (b) An illustration of lifting the momenta alignment due to curving of electron trajectories in external field.

Similarly, the second condition requires that $(\mathbf{P} \pm \mathbf{q}_1) \cdot \mathbf{Q} \sim \omega k_F / v_F$. Combining the two conditions, we have $|\epsilon_{\mathbf{q}_1+\mathbf{P}-\mathbf{Q}/2} - \epsilon_{\mathbf{q}_1-\mathbf{Q}/2}| \sim \omega$. The latter relation can be cast in the form $\mathbf{P} \cdot (2\mathbf{q}_1 + \mathbf{P} - \mathbf{Q}) \sim \omega k_F / v_F$. Since both scalar products $\mathbf{P} \cdot \mathbf{Q}$ and $\mathbf{P} \cdot \mathbf{q}_1$ are $\sim \omega k_F / v_F$, we arrive at the estimate $|\mathbf{P}| \sim |\mathbf{q}_1| \sim k_F (\omega / E_F)^{1/2}$. Therefore, the angle between the momenta within the first pair is small as $|\mathbf{q}_1|/k_F \sim (\omega/E_F)^{1/2}$. Similarly, the momenta within the second pair are aligned in the angular interval $\sim (\omega/E_F)^{1/2}$.

For the purpose of our derivation, we reformulate the above restriction in coordinate space, where ω defines the distance, r, between the subsequent scattering processes via the relation $\omega \sim v_F / r$. Correlation between the momenta implies that the three points, $\mathbf{r} = \mathbf{r}_1$, $\mathbf{r} = \mathbf{0}$, and $\mathbf{r} = \mathbf{r}_2$, in which creation, rescattering, and annihilation take place, are located close to the same straight line; see Fig. 1(b). The "tolerance" in the angle between the vectors $\mathbf{r}_1$ and $\mathbf{r}_2$, is the same as the degree of alignment in the momentum space; $\theta(r) \sim (1/k_F r)^{1/2}$.

In the presence of inhomogeneity, the Fermi momentum, $k_F = (2\pi n)^{1/2}$, becomes a function of coordinates. It is convenient to characterize the random spatial variations of $n(\mathbf{r})$ by a random force field, $\mathbf{F}(\mathbf{r})$, related to the local density gradient as $\nabla n(\mathbf{r})/\langle n \rangle = e\mathbf{F}(\mathbf{r})/E_F$, where $\langle n \rangle$ is the average density. Denote with $D \gg k_F^{-1}$ and $\delta n \ll \langle n \rangle$ the characteristic scale and the magnitude of the density fluctuations. Then the typical value of the force is $F \sim (E_F/eD)(\delta n/\langle n \rangle)$. The force, $\mathbf{F}(r)$, curves slightly the classical electron trajectories, transforming them into arcs with curving angle $\theta_F = eF_\perp r / 2E_F$ [Fig. 1(b)], where $F_\perp$ is the component of force perpendicular to $\mathbf{r}$. Obviously, the process represented by the diagram in Fig. 1(a) gets suppressed as θ_F exceeds $\theta(r)$. The condition $\theta_F = \theta(r)$ defines the characteristic distance

$$r_0 \sim k_F^{-1} (E_F k_F / eF)^{2/3} \tag{1}$$

and the corresponding energy scale

$$\omega_0 = v_F / r_0 \sim E_F (k_F D)^{-2/3} [\delta n / \langle n \rangle]^{2/3}. \tag{2}$$

The latter scale is the energy width of the feature, $\delta\nu(\omega)$, in the tunnel density of states. As seen from Eq. (2), this scale is determined by the characteristics of the density variations in combination $(\delta n/D)^{2/3}$.

The scales r_0 and ω_0 can be derived qualitatively from a different reasoning. The phase acquired by the electron upon traveling the distance r is $\phi(r) = k_F r$. Elongation, $\delta\mathcal{L}$, of the trajectory due to curving, results in additional phase $\delta\phi(r) = k_F \delta\mathcal{L} = k_F r(\theta_F - \sin\theta_F)/\theta_F \sim k_F r \theta_F(r)^2$, where the curving angle, $\theta_F(r)$, was determined above. Curving becomes important when $\delta\phi(r) \sim \pi$. This condition yields the same $r = r_0$ as given by Eq. (1).

In the above consideration we assumed that the force does not change within the characteristic distance, r_0, between the collisions. The corresponding condition, $r_0 \ll D$, can be cast in the form

$$\frac{r_0}{D} = \frac{1}{k_F D} \left(\frac{E_F k_F}{eF} \right)^{2/3} \sim \frac{(\langle n \rangle D^2)^{1/2}}{(\delta n D^2)^{2/3}} \ll 1. \tag{3}$$

Equation (3) requires that the density variations are very smooth, $D \gg \langle n \rangle^{3/2}/(\delta n)^2$. The other point to be checked is whether the language of the smooth variations of local density, $n(\mathbf{r})$, that we have used, is adequate. Position-dependent $n(\mathbf{r})$ can be introduced if the statistical fluctuation, $(\langle n \rangle D^2)^{1/2}$, is smaller than the change, $\delta n D^2$, of the number of electrons within the correlation area, D^2, due to the smooth fluctuations. It is seen from Eq. (3) that our main condition $r_0 \ll D$ is stronger than the condition $\delta n D^2 \gg (\langle n \rangle D^2)^{1/2}$, so that the reasoning within the language of local density fluctuations is justified.

It is also instructive to compare the width, ω_0, with characteristic spatial change of the potential energy of the electrons, $U = E_F \delta n / \langle n \rangle$. As seen from Eq. (2)

$$\omega_0 / U \sim (\delta n D^2)^{-1/3} \ll 1, \tag{4}$$

so that the anomaly is much narrower than the variation of the chemical potential. Concerning the magnitude, $\delta\nu_0 = \delta\nu(\omega_0)$, of the anomaly, we will establish that

$$\frac{\delta\nu_0}{\nu} \sim \left(\frac{\omega_0}{E_F} \right)^{3/2} \sim \frac{\delta n D^2}{(\langle n \rangle D^2)^{3/2}} \gg \frac{1}{(\langle n \rangle D^2)^{3/4}} \tag{5}$$

in the course of the calculation, to which we turn.

Green functions.—Finding the functional form of $\delta\nu(\omega)$ amounts, essentially, to evaluation of the diagram Fig. 1(a) in the coordinate space with account of the random (but locally homogeneous) field, $\mathbf{F}$. This field enters into the electron Green function

$$G_\Omega(0, \mathbf{r}) = \frac{i^{1/2}\nu}{\sqrt{2\pi k_F r}} \exp\left\{ \frac{i\Omega r}{v_F} + i k_F r + i\delta\phi(0, \mathbf{r}) \right\} \tag{6}$$

in coordinate-energy space via the additional phase

$$\delta\phi(0, \mathbf{r}) = \int_0^r k(\mathbf{r}) dl - k_F r, \tag{7}$$

where $k(\mathbf{r})$ is the wave vector along the classical trajectory, connecting the points 0 and $\mathbf{r}$. Suppose that $\mathbf{r}$ is directed along the x axis. The parabolic trajectory is

$$y(x) = F_y x(r - x)/4E_F, \tag{8}$$

while $dl = dx\sqrt{1 + (dy/dx)^2} \approx dx\sqrt{1 + \frac{1}{2}(dy/dx)^2}$. This allows us to rewrite Eq. (7) in the form

$$\delta\phi(0, \mathbf{r}) = \frac{k_F}{2} \int_0^r dx \left(\frac{dy}{dx} \right)^2 + \int_0^r dx \{ k[y(x)] - k_F \}. \tag{9}$$

Substituting Eq. (8) into Eq. (9) and using the relation $\partial k / \partial y = [k_F F_y y(x)]/(2E_F)$, we find

$$\delta\phi(0, \mathbf{r}) = -k_F F_y^2 r^3 / 96 E_F^2 = -k_F r \theta_F^2 / 24, \tag{10}$$

which, within a numerical factor, coincides with the above qualitative estimate. Naturally, the x component of the field

also contributes to $\delta\phi$. However, this contribution gauges out in the expression for $\delta\nu(\omega)$.

Density of states.—The analytical expression corresponding to the diagram Fig. 1(a) in the coordinate space reads

$$\delta\nu(\omega) = \mathrm{Im}\frac{2iV^3}{\pi^2\nu^3}\int\frac{d\Omega}{2\pi}\int d\mathbf{r}d\mathbf{r}_1 d\mathbf{r}_2 G_\Omega(\mathbf{r},\mathbf{r}_1)G_\omega(\mathbf{r}_1,\mathbf{r}_2)\Pi_{\omega-\Omega}(\mathbf{r}_1,0)\Pi_{\omega-\Omega}(0,\mathbf{r}_2)G_\omega(\mathbf{r}_2,\mathbf{r}), \tag{11}$$

where the polarization operator, $\Pi_\Omega(\mathbf{r},\mathbf{r}')$, is defined as

$$\Pi_\Omega(\mathbf{r},\mathbf{r}') = -i\int\frac{d\Omega'}{2\pi}G_{\Omega'}(\mathbf{r},\mathbf{r}')G_{\Omega-\Omega'}(\mathbf{r}',\mathbf{r}) \tag{12}$$

and V is the dimensionless (multiplied by ν) Fourier component of the interaction potential, which we assume to be short-range. We are interested in the oscillatory part of the polarization operator in the presence of the external field. Substituting Eq. (6) into Eq. (12), we readily obtain for this part

$$\Pi_\Omega(0,\mathbf{r}) = -\frac{\nu}{2\pi r^2}\sin[2k_F r - 2\delta\phi(\mathbf{r})]\exp\left\{i\frac{\Omega r}{v_F}\right\}. \tag{13}$$

In Eq. (11) the integration over azimuthal angles of $\mathbf{r}_1$ and $\mathbf{r}_2$ can be performed analytically, using the relation $\langle\exp[i\mathbf{p}\cdot(\mathbf{r}_1+\mathbf{r}_2)]\rangle_{\varphi_p,\varphi_{r_1},\varphi_{r_2}} = \sin[p(r_1\pm r_2)+\pi/4]/p(r_1 r_2)^{1/2}$. Also, the integration over $\mathbf{r}$ can be carried out explicitly with the help of the identity $\int d\mathbf{r}G_\Omega(\mathbf{r}_1,\mathbf{r})\times G_\Omega(\mathbf{r},\mathbf{r}_2) = \partial G_\Omega(\mathbf{r}_1,\mathbf{r}_2)/\partial\Omega$. Upon performing these integrations and combining rapidly oscillating terms in the integrand of Eq. (11) into "slow," oscillating with period $\gg k_F^{-1}$, terms, we obtain

$$\begin{aligned}\delta\nu(\omega) = -\frac{\nu V^3}{2E_F\pi^{3/2}k_F^{1/2}}&\int_{r_2>r_1}\frac{dr_1 dr_2}{(r_1 r_2)^{3/2}}\\ &\times\int_0^\omega d\Omega\sin[v_F^{-1}(\omega-\Omega)(r_1+r_2)]\\ &\times\sum_\pm(r_2\pm r_1)^{1/2}\sin[r_1 r_2(r_2\pm r_1)/r_0^3\\ &+\pi/4\mp v_F^{-1}(\omega+\Omega)(r_2\pm r_1)],\end{aligned} \tag{14}$$

where $r_0 = (2^{4/3}/k_F)(E_F k_F/eF_y)^{2/3}$. It is seen that the characteristic scale of distances r_1, r_2 in the integral Eq. (14) is indeed equal to r_0 in accordance with qualitative consideration [see Eq. (1)]. The origin of the combinations $r_1 r_2(r_2\pm r_1)/r_0^3$ can be understood from Fig. 1(b). The scattering sequence $\mathbf{r}_1\to\mathbf{0}\to\mathbf{r}_2\to\mathbf{r}_1$ leads to the accumulation of the field-dependent phase $2[\delta\phi(r_1)+\delta\phi(r_2)-\delta\phi(|\mathbf{r}_2-\mathbf{r}_1|)]$. The above combinations emerge from this additional phase upon using Eq. (10). Two contributions to the integral Eq. (14) correspond to the locations of the points $\mathbf{r}_1$ and $\mathbf{r}_2$ on the opposite and the same sides of the origin, respectively.

The shape of the anomaly.—The remaining task is to perform the Gaussian averaging over the random field, F. Since $r_0^{-3}\propto F_y^2$, this averaging can be performed inside the integrand of Eq. (14) with the help of the identity

$$\int_{-\infty}^{\infty}dx e^{-x^2}\cos(\alpha x^2+\beta) = H_1(\alpha)\cos\beta - H_2(\alpha)\sin\beta, \tag{15}$$

where the functions H_1 and H_2 are defined as follows:

$$H_{1,2}(\alpha) = (\pi/2)^{1/2}\sqrt{(1+\alpha^2)^{-1/2}\pm(1+\alpha^2)^{-1}}. \tag{16}$$

We present the final result in the form $\delta\nu(\omega)/\nu = A\Phi(\omega/\omega_0)$, with

$$\omega_0 = E_F\left[\frac{e\langle F^2\rangle^{1/2}}{\sqrt{2}E_F k_F}\right]^{2/3} = \frac{E_F\langle(\nabla n)^2\rangle^{1/3}}{(4\pi)^{1/3}\langle n\rangle}, \tag{17}$$

in agreement with qualitative estimate Eq. (2), and with constant A defined as

$$A = -\frac{V^3 v_F}{4\pi E_F k_F^{1/2} r_0^{3/2}} = -\frac{V^3}{8\sqrt{2}\pi^{3/2}}\left[\frac{\langle(\nabla n)^2\rangle}{\langle n\rangle^3}\right]^{1/2}; \tag{18}$$

the dimensionless function, $\Phi(z)$, describing the shape of the anomaly, is given by

$$\begin{aligned}\Phi(z) = &\int_{\rho_2>\rho_1}\frac{d\rho_1 d\rho_2}{(\rho_1\rho_2)^{3/2}}\int_0^z dz'\sin[(z-z')(\rho_1+\rho_2)]\\ &\times\{S_+(\rho_1,\rho_2)+C_+(\rho_1,\rho_2)+S_-(\rho_1,\rho_2)\\ &+C_-(\rho_1,\rho_2)\}\\ &= \Phi_+(z)+\Phi_-(z),\end{aligned} \tag{19}$$

where the functions S_+, S_-, C_+, and C_- are defined as

$$\begin{aligned}S_\pm(\rho_1,\rho_2) = (\rho_1\pm\rho_2)^{1/2}&\sin\left[\frac{\pi}{4}\mp(z+z')(\rho_1\pm\rho_2)\right]\\ &\times\{H_1(\rho_1\rho_2(\rho_1\pm\rho_2))-\sqrt{\pi}\},\end{aligned} \tag{20}$$

$$\begin{aligned}C_\pm(\rho_1,\rho_2) = (\rho_1\pm\rho_2)^{1/2}&\cos\left[\frac{\pi}{4}\mp(z+z')(\rho_1\pm\rho_2)\right]\\ &\times H_2(\rho_1\rho_2(\rho_1\mp\rho_2)).\end{aligned} \tag{21}$$

In definitions of S_+ and S_- we had subtracted from the function $H_1(\alpha)$ the zero-F value $H_1(0)=\sqrt{\pi}$. Integration over z' in Eq. (19) can be carried out analytically. The remaining integrals over ρ_1, ρ_2 were evaluated numerically. The resulting shape of the zero-bias anomaly is shown in Fig. 2. The small $z\ll 1$ behavior of $\Phi(z)$ is $8\ln z$; i.e., it diverges logarithmically. The cutoff is chosen from the condition that $\Phi(z)$ approaches zero at large z. Note, that $\Phi(z)$ exhibits a pronounced feature around $z=1$. The origin of this feature lies in strong oscillations of the integrand in Eq. (14). The "trace" of these oscillations survives after averaging over the magnitude of the random

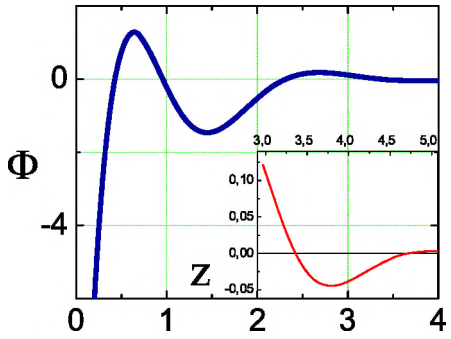

FIG. 2 (color online). Dimensionless function, $\Phi(z)$, describing the shape of the zero-bias anomaly is plotted from Eq. (19) versus dimensionless energy $z = \omega/\omega_0$. Inset in the lower right corner: enlarged plot of $\Phi(z)$ in the domain $3 < z < 5$.

field. In fact, the oscillations persist beyond $z = 3$, as seen in the inset in Fig. 2. Also, analytical inspection of Eq. (19) for $z \gg 1$ yields

$$\Phi_+(z)|_{z\gg 1} \approx -2^{3/4}\sqrt{\pi}\,\frac{\sin(2^{8/3}\sqrt{3}z)}{z^{3/4}}\exp\{-2^{8/3}z\}. \quad (22)$$

Other third-order processes.—Equations (17)–(19) were derived for a specific process, illustrated in the diagram in Fig. 1(a). However, creation, rescattering, and annihilation of a pair can follow a different scenario; e.g., the rescattering process can involve the initial electron, as illustrated by the second and third diagrams in Fig. 3. It is important that the restriction concerning the momenta alignment, leading to the zero-bias anomaly, applies to this scenario as well. It also applies to all other diagrams in Fig. 3. Note that diagrams in Fig. 3 do not exhaust possible third-order processes [6]. All contributions to $\delta\nu$ of the diagrams in Fig. 3 have the same analytical structure and differ only by numerical coefficients, originating from spin degeneracy and from closed fermion loops [each bringing a factor (-2)]. Collecting these contributions amounts to multiplying the first diagram in Fig. 3 by $1/2$.

Concluding remarks.—Higher-order processes in a homogeneous electron gas, involving $n > 2$ electron-hole pairs, are also subject to the momenta restriction [6], leading to the anomaly in the presence of inhomogeneity. However, these processes are suppressed as $(\omega_0/E_F)^{n/2}$ due to the phase-space limitation.

Note that in addition to the oscillating term, the polarization operator Eq. (13) also contains a slow-varying term $\propto |\Omega|/r$. Evaluating $\delta\nu(\omega)$ from Eq. (11) with this slow part of Π_Ω yields a nonanomalous correction. The same applies to all diagrams in Fig. 3.

In experimental situations, the electrons are supplied to the 2D gas by donor impurities, separated from electrons by a wide spacer. Growth-related technological inhomogeneities, like ridges [7], do not change the average electron density, but redistribute electrons over the plane [8] and set

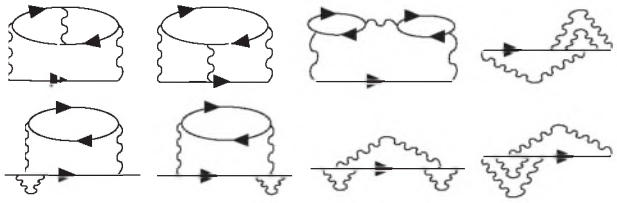

FIG. 3. Diagrams representing all third-order processes with aligned momenta of the virtual states.

scales δn and D. In principle, individual donors themselves create the Friedel oscillations of the electron density. However, these oscillations are exponentially suppressed due to the large separation of donors from the 2D gas. A question might be asked as to why in evaluating diagram in Fig. 1(a) we neglected violation of the momentum conservation due to the impurity scattering. The answer is that condition Eq. (3) justifies such neglect. This is because at distances larger than the Bohr radius, the donor potential is screened. Thus, instead of individual donors, the electron is scattered by a smooth in-plane potential with spatial scale D. Then the scattering angle does not exceed $1/(k_F D)$. On the other hand, the relevant curving angle, θ_F, is $(\omega_0/E_F)^{1/2} \sim [(\delta n/n)]^{1/3}(k_F D)^{-1/3}$, as follows from Eq. (2). Condition Eq. (3) guarantees that this angle is bigger than $1/(k_F D)$. Summarizing, borrowing momentum from donors is not efficient, since they are distant and screened.

This conclusion is also supported by comparison of the inverse transport scattering time, $\tau_{tr}^{-1} \sim E_F(U/E_F)^2 \times (1/k_F D)$, from screened impurities and the energy scale ω_0. As follows from Eq. (2) the ratio $1/(\omega_0\tau_{tr}) \sim (U/E_F)^{4/3}(1/k_F D)^{1/3}$ is small. The latter also implies that the diffusive anomaly of Ref. [2] develops at ω much smaller than ω_0.

Discussions with A. Andreev, A. Chubukov, L. Glazman, B. Halperin, D. Maslov, and K. Matveev are gratefully acknowledged. E. M. acknowledges the support of DOE Grant No. DE-FG02-06ER46313.

[1] B. L. Altshuler and A. G. Aronov, Solid State Commun. **30**, 115 (1979).
[2] B. L. Altshuler, A. G. Aronov, and P. A. Lee, Phys. Rev. Lett. **44**, 1288 (1980).
[3] A. M. Rudin, I. L. Aleiner, and L. I. Glazman, Phys. Rev. B **55**, 9322 (1997).
[4] D. V. Khveshchenko and M. Reizer, Phys. Rev. B **57**, R4245 (1998).
[5] E. G. Mishchenko and A. V. Andreev, Phys. Rev. B **65**, 235310 (2002).
[6] S. Gangadharaiah *et al.*, Phys. Rev. Lett. **94**, 156407 (2005); A. V. Chubukov *et al.*, *ibid.* **95**, 026402 (2005); Phys. Rev. B **71**, 205112 (2005).
[7] R. L. Willett *et al.*, Phys. Rev. Lett. **87**, 126803 (2001).
[8] N. B. Zhitenev *et al.*, Nature (London) **404**, 473 (2000).